Infrared Multiphoton Dissociation Spectroscopy of a Gas-Phase Complex of Uranyl and 3-Oxa-Glutaramide: An Extreme Red-Shift of the [O═U═O]²⁺ Asymmetric Stretch

John K. Gibson,*,[†] Han-Shi Hu,[‡] Michael J. Van Stipdonk,[§] Giel Berden,[∥] Jos Oomens,[∥,⊥] and Jun Li*,[‡,#]

[†]Chemical Sciences Division, Lawrence Berkeley National Laboratory, 1 Cyclotron Road, Berkeley, California 94720, United States

[‡]Department of Chemistry & Laboratory of Organic Optoelectronics and Molecular Engineering of the Ministry of Education, Tsinghua University, Beijing 100084, China

[§]Department of Chemistry and Biochemistry, Duquesne University, 600 Forbes Avenue, Pittsburgh Pennsylvania 15282, United States

[∥]Institute for Molecules and Materials, FELIX Laboratory, Radboud University Nijmegen, Toernooiveld 7, 6525ED Nijmegen, The Netherlands

[⊥]van 't Hoff Institute for Molecular Sciences, University of Amsterdam, Science Park 904, 1098XH Amsterdam, The Netherlands

[#]William R. Wiley Environmental Molecular Sciences Laboratory, Pacific Northwest National Laboratory, Richland, Washington 99352, United States

ABSTRACT: The gas-phase complex $UO_2(TMOGA)_2^{2+}$ (TMOGA = tetramethyl-3-oxa-glutaramide) prepared by electrospray ionization was characterized by infrared multiphoton dissociation (IRMPD) spectroscopy. The IRMPD spectrum from 700–1800 cm^{-1} was interpreted using a computational study based on density functional theory. The predicted vibrational frequencies are in good agreement with the measured values, with an average deviation of only 8 cm^{-1} (<1%) and a maximum deviation of 21 cm^{-1} (<2%). The only IR peak assigned to the linear uranyl moiety was the asymmetric ν_3 mode, which appeared at 965 cm^{-1} and was predicted by DFT as 953 cm^{-1}. This ν_3 frequency is red-shifted relative to bare uranyl, UO_2^{2+}, by ca. 150 cm^{-1} due to electron donation from the TMOGA ligands. Based on the degree of red-shifting, it is inferred that two TMOGA oxygen-donor ligands have a greater effective gas basicity than the four monodentate acetone ligands in $UO_2(acetone)_4^{2+}$. The uranyl ν_3 frequency was also computed for uranyl coordinated by two TMGA ligands, in which the central O_{ether} of TMOGA has been replaced by CH_2. The computed ν_3 for $UO_2(TMGA)_2^{2+}$, 950 cm^{-1}, is essentially the same as that for $UO_2(TMOGA)_2^{2+}$, suggesting that electron donation to uranyl from the O_{ether} of TMOGA is minor. The computed ν_3 asymmetric stretching frequencies for the three actinyl complexes, $UO_2(TMOGA)_2^{2+}$, $NpO_2(TMOGA)_2^{2+}$ and $PuO_2(TMOGA)_2^{2+}$, are comparable. This similarity is discussed in the context of the relationship between ν_3 and intrinsic actinide-oxygen bond energies in actinyl complexes.

$UO_2(TMOGA)_2^{2+}$
O═U═U
ν_3 = 965 cm^{-1}
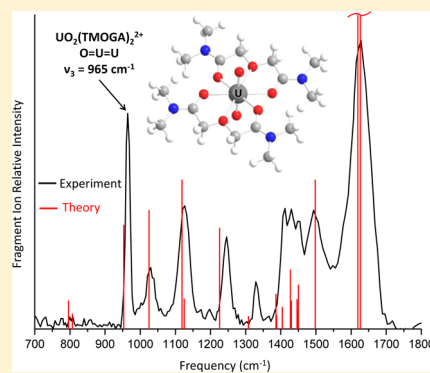
— Experiment
— Theory

INTRODUCTION

The uranyl moiety, UO_2^{2+}, is ubiquitous in uranium chemistry, and its chemical and physical characteristics in both the condensed and gas phases have been considered in detail by using experiment and theory.[1−15] The infrared (IR) active asymmetric ν_3 stretching mode of uranyl has been studied extensively in both condensed and gas phases, with a focus on the effect of ligation on the frequency. In aqueous solution, the hydrated uranyl ν_3 frequency is close to 963 cm^{-1}.[16−19] In solutions comprising basic ligands, and in solid complexes, the ν_3 frequency is red-shifted into the range of ca. 850 to 950 cm^{-1},[19−25] depending on the coordination environment. The general conclusion is that more electron-donating ligands generally have a greater red-shifting effect for this uranyl frequency.[17] Vallet et al. have concluded that the uranyl bond is destabilized due to charge donation and that this effect is primarily electrostatic, rather than due to a reduction in covalent bonding.[26] In addition to the computational complexities in condensed phase, effective detailed interpretation of uranyl frequency shifts in solution are hampered by uncertainties in the actual solution coordination; Bühl et al. have demonstrated that in solution uranyl is coordinated by water rather than by the stronger base acetonitrile.[27]

As an alternative to complex condensed phase environments that are difficult to accurately model, the properties of uranyl complexes can be studied in cryogenic matrices or in the gas phase. Andrews and co-workers reported ν_3 values for neutral UO_2 of 776.0 and 914.8 cm^{-1} in solid argon and neon, respectively,[28−30] and ν_3 values in the range of 980.1−929.0 cm^{-1} for cationic UO_2^+ in xenon, krypton, argon, and neon

matrices;[31] however, they were unable to obtain a frequency for uncoordinated UO_2^{2+}.[28] The first correlation of gas-phase uranyl vibrational frequencies and ligation was performed by Bray and Kramer.[22] They obtained IR spectra for neutral uranyl hexafluoroacetylacetonate (hfac) adducts with additional basic ligands. The bare complex, which can simplistically be formulated as $UO_2^{2+}(hfac^-)_2$, exhibited a ν_3 of 958 cm^{-1}. Addition of increasingly basic ligands red-shifted this value to 950 cm^{-1} for hexamethylphosphoramide, which has a very high gas basicity (GB) of 929 kJ/mol.[32] The rather small red-shift upon addition of neutral basic ligands to $UO_2^{2+}(hfac^-)_2$ reflects that the uranyl moiety is effectively coordinated by the two hfac anion ligands and is minimally perturbed by the addition of secondary neutral ligands. More recently, IR spectra have been acquired for several gas-phase anionic complexes of uranyl, such as $UO_2(NO_3)_3^-$.[33−35] The ν_3 frequencies of these complexes are generally comparable to those of the same species in solution, reflecting similarly strong and saturated coordination of the uranyl cation by anion ligands in both media.

A central goal in the chemistry of uranyl is to ascertain and understand the effects of ligation by Lewis base ligands on the uranium−oxygen bonds. Infrared multiphoton dissociation (IRMPD) spectroscopy of gas-phase $UO_2(L)_n^{2+}$ complexes, where L is a neutral Lewis base ligand, is an effective approach for probing perturbations to the bonding in uranyl; the ν_3 asymmetric frequency can be used as a diagnostic of changes in the U−O bonds. In contrast to solution species, mass-selected gas-phase complexes have a definitive composition and furthermore are not perturbed by secondary solvation effects, which renders them amenable to accurate theoretical modeling. Groenewold et al. have obtained the first IRMPD spectra for $UO_2(L)_n^{2+}$,[36] employing the ion cyclotron resonance mass spectrometer at the high intensity Free Electron Laser for Infrared eXperiments (FELIX) facility.[37] The measured ν_3 were red-shifted from the predicted value of ∼1100 cm^{-1} for bare UO_2^{2+} to 1017, 1000, and 988 cm^{-1} for n = 2, 3, and 4, respectively in $UO_2(acetone)_n^{2+}$. Charge donation from the acetone ligands (GB = 782 kJ/mol[32]) results in red-shifting of the asymmetric stretching frequency, which is interpreted as reflecting a weakening of the U−O bonds.[26,36,38] Less red-shifts were observed for $UO_2(acetonitrile)_n^{2+}$ complexes, in accord with the lower GB[acetonitrile] = 748 kJ/mol.[32] $UO_2(water)_n^{2+}$ complexes could not be prepared by electrospray ionization (ESI) under the ESI conditions at FELIX due to the low GB[water] = 660 kJ/mol.[32] The lowest measured ν_3, 988 cm^{-1} for $UO_2(acetone)_4^{2+}$, is substantially higher than ν_3 for uranyl anion complexes such as $UO_2(NO_3)_3^-$ (ν_3 = 949 cm^{-1});[33] neutral Lewis base ligands predictably do not perturb the uranyl moiety to the degree that extremely basic anion ligands do.

The ability to perturb the UO_2^{2+} moiety by coordination of neutral electron-donating Lewis base ligands can be further explored by both experiment and complementary theory. Issues include establishing a more complete relationship between the GB of ligands and the degree of red-shifting of ν_3, the degree to which ν_3 can be red-shifted by neutral Lewis base ligands, and the underlying basis for these changes in frequencies. If the interpretation that the degree of red-shifting is directly related to the weakening of the uranium-oxo bonds in uranyl, then it should be possible to probe this effect by reactivity, such as oxo-exchange in which the U−O bonds must be activated.[39]

In this paper we report on an experimental and theoretical study of the vibrational spectrum of a complex of uranyl with tetramethyl-3-oxa-glutaramide (TMOGA), $UO_2(TMOGA)_2^{2+}$.

TMOGA is a model separations ligand,[40−43] which has been shown to also very effectively coordinate metal ions in the gas phase.[44,45] The structure of the TMOGA ligand is shown in Figure 1, where the C−O bond cleavage that occurs in collision
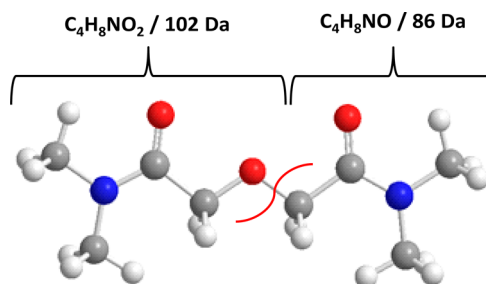

C$_4$H$_8$NO$_2$ / 102 Da   C$_4$H$_8$NO / 86 Da

Figure 1. Structure of TMOGA showing the C−O ether bond cleavage that appears in the IRMPD spectrum.

induced dissociation is indicated.[46] The previously reported computed structure of $UO_2(TMOGA)_2^{2+}$ is shown in Figure 2.[46] The formally tridentate TMOGA ligand strongly coordinates cations and has been shown to produce tetra-positive metal ion complexes, An(TMOGA)$_3^{4+}$ by ESI (An = Th, U, Np, Pu).[44,45] Although the GB of TMOGA is not known, it can be inferred that it must be very high to achieve stabilization of tetrapositive metal ions from solution to gas. In the present study, we report the observed and computationally predicted IR spectra of $UO_2(TMOGA)_2^{2+}$, with a particular emphasis on the extraordinary red-shift of the uranyl ν_3 band in this complex. Comparison is made among the computed ν_3 frequencies for $UO_2(TMOGA)_2^{2+}$, $NpO_2(TMOGA)_2^{2+}$, and $PuO_2(TMOGA)_2^{2+}$ to evaluate bonding trends across the actinyl series with a focus on the intrinsic bond dissociation energies.

■ EXPERIMENTAL METHODS

Using a stock solution of 10 mM uranyl perchlorate in water, a solution of approximately 1 mM UO_2^{2+} and 4 mM TMOGA in 90% methanol/10% water was prepared for ESI in the IRMPD experiments. Previously established methods for generation of ions and the subsequent collection of IRMPD spectra were used here.[33−36,47−49] Briefly, ESI was performed using a Micromass (now a component of Waters Corporation, Milford MA) Z-Spray source. Dry nitrogen (∼80 °C) was used to assist in the desolvation process. Ions were injected into a home-built Fourier transform ion cyclotron resonance (FT-ICR) mass spectrometer described in detail elsewhere.[37] Ions were accumulated for the duration of the previous FT-ICR cycle (6 s) in an external hexapole and injected into the ICR cell via a quadrupole deflector and an octapole RF ion guide. Instrument operating parameters, such as desolvation temperature, cone voltage, and ion accumulation and transfer optics voltages, were optimized to maximize formation of $UO_2(TMOGA)_2^{2+}$ ions and transfer of the species to the ICR cell.

Infrared spectra were recorded by measuring the photo-dissociation yield as a function of photon wavelength. Precursor ions were irradiated using 25 FELIX macropulses (55 mJ per macropulse, 5 μs pulse duration, fwhm bandwidth ∼0.5% of central λ). In the IRMPD process, a photon is absorbed when the laser frequency matches a vibrational mode of the gas-phase ion and its energy is subsequently distributed over all vibrational modes by intramolecular vibrational redistribution
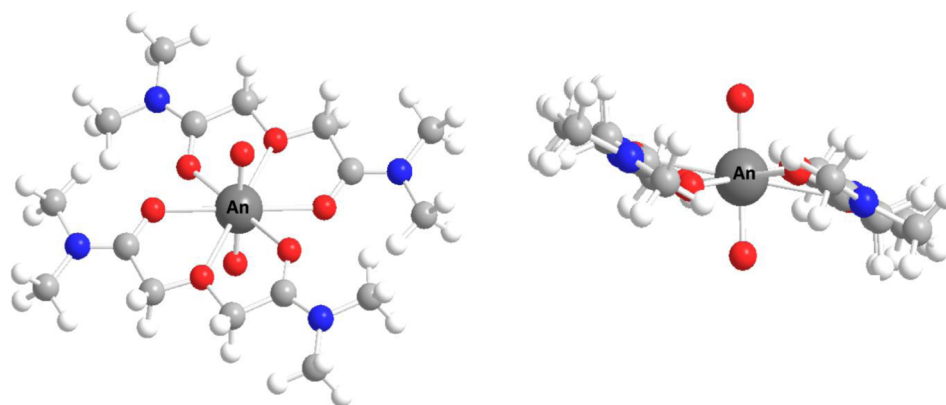
Figure 2. Computed structures of gas-phase $AnO_2(TMOGA)_2^{2+}$ complexes (from ref 46).

(IVR).[50] The IVR process allows the energy of each photon to be dissipated before the ion absorbs another, which leads to promotion of ion internal energy toward the dissociation threshold via multiple photon absorption.[67] Infrared spectra obtained using IRMPD are comparable to those collected using linear absorption techniques.[51,52] For these experiments, the FEL wavelength was tuned between 5.6 (1800 cm^{-1}) and 14 μm (700 cm^{-1}) in 5 cm^{-1} increments. The intensities of product and undissociated precursor ions were obtained from an averaged mass spectrum measured using the excite/detect sequence of the FT-ICR-MS after each IRMPD step. The IRMPD yield was normalized to the total ion current and linearly normalized for variations in the laser intensity.

COMPUTATIONAL DETAILS

The computational details have been provided previously[46] and are only summarized here. The theoretical calculations of the $UO_2(TMOGA)_2^{2+}$, $NpO_2(TMOGA)_2^{2+}$, and $PuO_2(TMOGA)_2^{2+}$ complexes were carried out using spin-unrestricted Kohn−Sham density functional theory (DFT).[53,54] The local density approach (LDA)[55,56] and generalized gradient approach with PBE exchange-correlation functional[57] were used as implemented in the Amsterdam Density Functional program (ADF 2010.01).[58−60] Scalar relativistic (SR) effects were taken into account using the zero-order regular approximation (ZORA).[61] The frozen core approximation was applied to the [1s^2-5d^{10}] cores of U, Np, and Pu, and [1s^2] cores of C, N, and O, with the rest of the electrons explicitly treated variationally. The uncontracted Slater basis sets with quality of triple-ζ plus two polarization functions (TZ2P) were used for the valence electrons.[62] All the geometries were fully optimized with molecular symmetries and are shown to have all real vibrational frequencies. The vibrational frequencies were computed analytically, and zero-point energy (ZPE) corrections were included in the calculations of relative energies.

RESULTS AND DISCUSSION

Measured and Computed IR Spectra for $UO_2(TMOGA)_2^{2+}$. The experimental and computed IR spectra for $UO_2(TMOGA)_2^{2+}$ are shown in Figure 3. The computed peak intensities do not seem to correlate well with the observed intensities, as is typical for DFT calculations with harmonic approximations. However, the computed unscaled frequencies are in good agreement with the measured frequencies. The comparison between observed and predicted frequencies is summarized in Table 1; the peak assignments are in Table 2. It
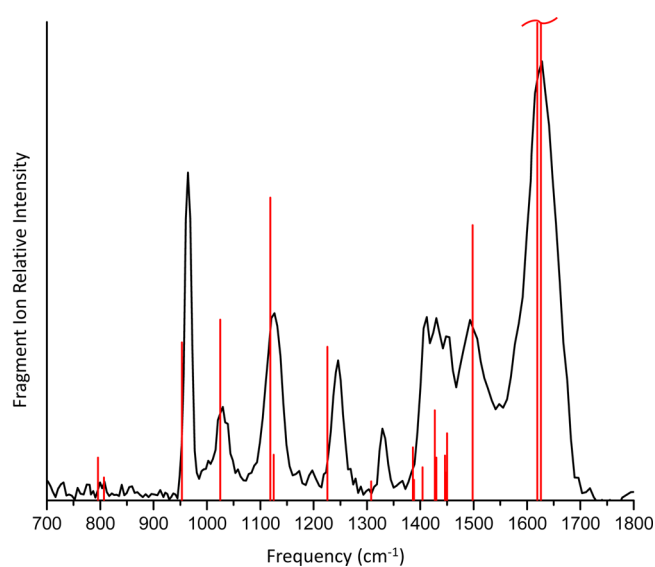

Figure 3. IRMPD spectrum of $UO_2(TMOGA)_2^{2+}$. The red lines indicate the computed frequencies (not scaled) and relative intensities (Table 2); the computed intensities of the modes at 1619 and 1626 cm^{-1} are off-scale, respectively 2.4 and 2.9 times greater than the indicated full-scale intensities.

Table 1. Experimental and Computed IR Frequencies for $UO_2(TMOGA)_2^{2+a}$

experimental	computed	Δ^b
965	953	12 [1.2]
1030	1024	5 [0.5]
1126	1119, 1125^c	4 [0.4]
1246	1226	20 [1.6]
1329	1308	21 [1.6]
1412	1404	8 [0.6]
1430	1427, 1430^c	−2 [0.1]
1448	1446, 1449, 1450^c	0 [0]
1493	1498	−5 [0.3]
1628	1619, 1626^c	6 [0.4]

^{a}Only the experimentally observed frequencies (cm^{-1}) are included. Additional computed frequencies, along with their intensities and assignments, are in Table 2. $^b\Delta$ is the difference Experimental − Computed (cm^{-1}). The computed values have not been scaled. The percent difference is given in brackets. ^{c}Peaks are too close to experimentally resolve.

Table 2. Computed Vibrational Mode Assignments, Frequencies and Intensities for $UO_2(TMOGA)_2^{2+a}$

mode assignment	$UO_2L_2^{2+}$
$H_3C-N-CH_3$ symmetric str./ $C-CH_2-O$ symmetric bend/UO_4 (equatorial oxygen) sym. bend (a_u)	795.6 (50)
$H_3C-N-CH_3$ symmetrical str./ $H_2C-O-CH_2$ symmetric str./ $C-CH_2-O$ antisymmetric str. (b_u)	806.6 (23)
$O-U-O$ asymmetric str. (b_u)	**953.2 (206)**
$H_2C-O-CH_2$ symmetric str. (b_u)	**1024.7 (237)**
$H_2C-O-CH_2$ asymmetric str. (a_u)	**1118.5 (402)**
$H_2C-O-CH_2$ asymmetric str./CH_3 wag. (a_u)	**1124.0 (54)**
$H_3C-N-CH_3$ asymmetric str. (a_u)	**1226.2 (200)**
CH_2 wag (a_u)	**1308.2 (18)**
CH_3 symmetric bend (umbrella) (b_u)	1386.4 (64)
CH_3 symmetric bend (umbrella) (a_u)	1387.8 (20)
CH_3/CH_2 symmetric bend (a_u)	**1403.9 (37)**
CH_3 asymmetric bend/CH_2 scissor (b_u)	**1426.6 (114)**
CH_3 asymmetric bend (b_u)	1430.4 (29)
CH_3 asymmetric bend/CH_2 scissor (a_u)	1430.4 (22)
CH_3 asymmetric bend (a_u)	1445.7 (22)
CH_3 asymmetric bend/CH_2 scissor (b_u)	1446.2 (32)
CH_3 asymmetric bend/CH_2 scissor (b_u)	1448.5 (30)
CH_3 asymmetric bend/CH_2 scissor (b_u)	1450.1 (84)
CH_3 asymmetric bend/CH_2 scissor (b_u)	**1497.7 (364)**
$O-C-N$ asymmetric str. (b_u)	**1618.8 (1498)**
$O-C-N$ asymmetric str. (a_u)	**1625.8 (1869)**

^{a}Frequencies are cm^{-1}. Intensities in parentheses are km/mol. The modes in bold were experimentally observed. Only modes with a computed intensity of ≥ 20 km/mol are included.

is seen from Table 1 that most of the predicted frequencies are within less than 1% of the measured value, and the maximum discrepancy is only 1.6%. It should be remarked that a "scaling factor" correction of 0.95–0.98 is typically employed to obtain good agreement between such experimental IR frequencies and those computed at the DFT/B3LYP level of theory; Groenewold et al. applied a scaling factor of 0.975 to the computed frequencies for $UO_2(L)_n^{2+}$ complexes.[36] The agreement here between the experimental and unscaled computed frequencies is unusually good, partly due to the use of PBE pure functional of the generalized gradient approach.

IRMPD mass spectra of $UO_2(TMOGA)_2^{2+}$ acquired off resonance at 1770 cm^{-1} and at the uranyl ν_3 absorption maximum at 965 cm^{-1} are shown in Figure 4. In the off-resonance spectrum, only peaks corresponding to the intact complex and instrumental electronic noise are apparent. The on-resonance spectrum exhibits four dominant fragment ions: $U^VO_2(TMOGA)^+$ (loss of a positively charged ligand); $U^{VI}O_2(TMOGA)(TMOGA-C_4H_8NO)^+$ (C−O bond cleavage shown in Figure 1); $U^VO_2^+$ (loss of a neutral and a positively charged ligand); and $U^{VI}O_2(TMOGA)(NC_2H_6)^+$ (N−C bond cleavage). The assigned oxidation states of uranium are based on whether the remaining ligands in the monopositive product are saturated (U^V) or radicals that bind to uranium to yield U^{VI}. The only positively charged TMOGA fragment was $C_4H_8NO^+$; other fragments were evidently ejected from the ICR cell upon dissociation. A minor IRMPD product corresponds to $UO_2(TMOGA-C_2H_6)^+$ (double N−C bond cleavage). Several of the minor product peaks could not be definitively assigned, reflecting the potential for diverse fragmentation channels for the TMOGA ligand. The IRMPD mass spectrum of $UO_2(TMOGA)_2^{2+}$ exhibits much more fragmentation than the low-energy collision induced dissociation spectrum, where

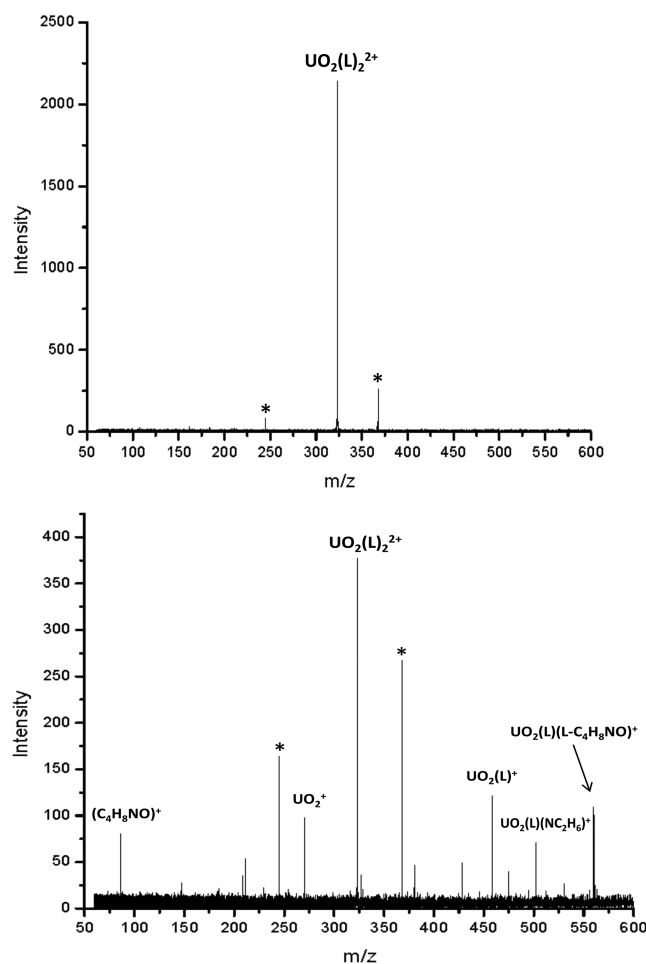**Figure 4.** IRMPD mass spectra for $UO_2(L)_2^{2+}$ (L = TMOGA) acquired off-resonance at 1770 cm^{-1} (top) and at the strong absorption at 965 cm^{-1} (bottom). The asterisked peaks are electronic noise. The dominant IRMPD fragments have been assigned; the peak at m/z 428 likely corresponds to $UO_2(TMOGA-C_2H_6)^+$.

$U^{VI}O_2(TMOGA)(TMOGA-C_4H_8NO)^+$ was overwhelmingly dominant and only minuscule $U^VO_2(TMOGA)^+$ was produced.[46]

The vibrational mode of particular interest here is the ν_3 asymmetric stretching frequency of the formally $[O=U=O]^{2+}$ moiety. As usual, the actual charge on uranyl in the complex is reduced below 2+ due to charge donation from the TMOGA ligands. Groenewold et al.[36] previously established a correlation between the ν_3 frequency and the degree of electron donation to the uranium metal center in uranyl coordination complexes. Vallet et al.[26] performed a computational study that reinforced the correlation between the ν_3 stretching frequency and the weakening of the uranium−oxygen axial bond due to charge donation. In the latter study the computed ν_3 for bare UO_2^{2+} was 1136 cm^{-1} and that for $UO_2(H_2O)_5^{2+}$ was 1028 cm^{-1}. As was found experimentally,[33,34] anionic ligands had a much greater effect on ν_3, with a predicted extreme shift to 832 cm^{-1} for $UO_2(OH)_4^-$.[26]

We focus here only on dipositive uranyl complexes with neutral donor ligands for comparison with the complex studied in the present work. The largest ν_3 red-shift reported by Groenewold et al. for gas-phase dipositive uranyl complexes was to 988 cm^{-1} for $UO_2(acetone)_4^{2+}$.[36] The ν_3 measured for $UO_2(TMOGA)_2^{2+}$ of 965 cm^{-1} indicates substantially more

electron donation from two tridentate TMOGA ligands than from four monodentate acetones, presumably due to the two coordinating ether oxygens in addition to the four ketone oxygens in TMOGA. The differences in ν_3 are as follows: $\Delta[UO_2(acetone)_2{}^{2+} - UO_2(acetone)_3{}^{2+}] = 17$ cm^{-1}; $\Delta[UO_2(acetone)_3{}^{2+} - UO_2(acetone)_4{}^{2+}] = 12$ cm^{-1}; $\Delta[UO_2(acetone)_2{}^{2+} - UO_2(acetone)_4{}^{2+}] = 29$ cm^{-1}; $\Delta[UO_2(acetone)_4{}^{2+} - UO_2(TMOGA)_2{}^{2+}] = 23$ cm^{-1}. The value of ν_3 for $UO_2(TMOGA)_2{}^{2+}$ is essentially the same as that for aqueous $UO_2{}^{2+}$, in which the uranyl is coordinated by five inner sphere water molecules,[63−65] this inner sphere coordination being the same as in $UO_2(H_2O)_5{}^{2+}$ for which the computed ν_3 is 1028 cm^{-1}.[26] The additional electron donation due to the bulk water environment beyond the five inner sphere water molecules in aqueous solution results in a substantial (>50 cm^{-1}) red-shift of the uranyl ν_3 frequency.

The GB of TMOGA is not yet known. From the proposed correlation between ν_3 and GB,[36] and the significantly greater red-shift in ν_3 for $UO_2(TMOGA)_2{}^{2+}$ versus $UO_2(acetone)_4{}^{2+}$, it can be inferred that the effective GB of a single TMOGA ligand is greater than that of two acetones. To further assess the origins of the extreme ν_3 red-shift for $UO_2(TMOGA)_2{}^{2+}$, computations were performed for the complex $UO_2(TMGA)_2{}^{2+}$ where TMGA is tetramethylglutamaride in which the central ether oxygen atom in TMOGA has been replaced by a CH_2 group; the schematic structure of the bidentate TMGA ligand and the computed structure of the $UO_2(TMGA)_2{}^{2+}$ complex are shown in Figure 5. The
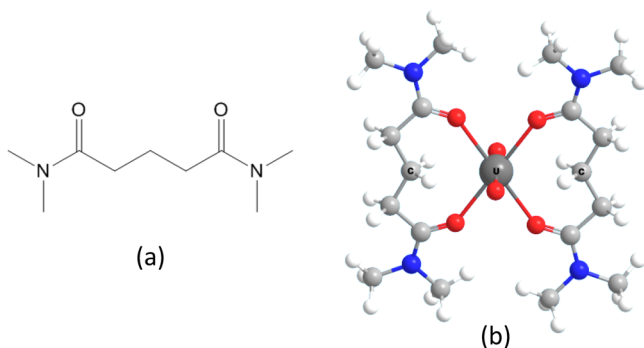

Figure 5. (a) Schematic structure of tetramethylglutamaride (TMGA); (b) Computed structure of $UO_2(TMGA)_2{}^{2+}$.

computed U−O$_{yl}$ and U−O$_{carbonyl}$ distances in $UO_2(TMGA)_2{}^{2+}$ are similar (1.78 and 2.45 Å, respectively) to those in $UO_2(TMOGA)_2{}^{2+}$ (1.78 and 2.38 Å). Most significantly, the computed ν_3 for $UO_2(TMGA)_2{}^{2+}$, 950 cm^{-1}, is essentially the same as that for $UO_2(TMOGA)_2{}^{2+}$, 953 cm^{-1}. This result implies that the ether oxygen atom in the TMOGA complex does not appreciably coordinate and contribute charge to the uranium metal center; in this regard the TMOGA complex can be considered as bidentate with the ether oxygen atom not significantly coordinating. In $UO_2(TMOGA)_2{}^{2+}$ the U−O$_{ether}$ distance, 2.77 Å, is significantly longer than the U−O$_{carbonyl}$ distance, 2.38 Å, such that the U−O$_{ether}$ interaction should be relatively minor, as the similarity between the computed ν_3 values for $UO_2(TMOGA)_2{}^{2+}$ and $UO_2(TMGA)_2{}^{2+}$ suggests. It should be noted that the U−O bond distances reported here are slightly longer than the previously optimized LDA distances, as is usual.[46] The TMOGA ligand can be considered as two dimethylformamide (DMF) ligands connected by a

$CH_2−O−CH_2$ linkage. The GB of DMF, 857 kJ/mol, is substantially greater than that of acetone, 782 kJ/mol;[32] the formamide moieties substantially enhance the Lewis acidity of the carbonyl oxygen atoms. Having concluded that the effective GB of TMOGA is greater than that of two acetones (GB[TMOGA] > 1564 kJ/mol), it can further be postulated that the GB of TMOGA is comparable to that of two DMFs, GB[TMOGA] $\approx$ 1714 kJ/mol. It may in the future be possible to test this hypothesis by measuring ν_3 for $UO_2(DMF)_4{}^{2+}$, which is predicted to exhibit a ν_3 close to that of $UO_2(TMOGA)_2{}^{2+}$. It would also be desirable to measure ν_3 for $UO_2(TMGA)_2{}^{2+}$ to confirm the predicted frequency. However, the excellent performance of theory in predicting ν_3 for $UO_2(TMOGA)_2{}^{2+}$ provides confidence in similar predictive reliability for $UO_2(TMGA)_2{}^{2+}$.

Asymmetric Stretching Frequencies for $AnO_2(TMOGA)_2{}^{2+}$ (An = U, Np, Pu). It was not practical to obtain experimental IRMPD spectra at FELIX for $NpO_2(TMOGA)_2{}^{2+}$ and $PuO_2(TMOGA)_2{}^{2+}$ due to the greater radiological hazards associated with the available isotopes for the synthetic elements Np and Pu. The IR spectra were, however, computed for all three actinyl complexes such that variations across the series can be made. The computed spectra for the neptunyl and plutonyl complexes are similar to those for the uranyl complex, with all three dominated by vibrational modes assigned to the equatorial TMOGA ligands. Of special interest are the comparative asymmetric actinyl ν_3 asymmetric stretching frequencies. The computed ν_3 values are 953 cm^{-1}, 959 and 955 cm^{-1} for $UO_2(TMOGA)_2{}^{2+}$, $NpO_2(TMOGA)_2{}^{2+}$ and $PuO_2(TMOGA)_2{}^{2+}$, respectively. These three similar values essentially parallel the known ν_3 for the actinyls in aqueous solution: 965 cm^{-1}, 969 and 962 cm^{-1} for $UO_2{}^{2+}$(aq), $NpO_2{}^{2+}$(aq) and $PuO_2{}^{2+}$(aq), respectively.[16] For both the TMOGA complexes and the aqueous ions, the three ν_3 are similar, with that for neptunyl being a few cm^{-1} higher than for the other two. Jones and Penneman correlated ν_3 for the three actinyls with the An-O force constants, k_{An-O}, obtaining values of 0.775 Mdyn/cm, 0.781 Mdyn/cm and 0.771 Mdyn/cm for uranyl, neptunyl and plutonyl, respectively.[16] Jones subsequently further rationalized the direct correlation between actinyl ν_3 and k_{An-O},[66] a result in accord with a recent theoretical assessment.[26] Rabinowitch has provided an evaluation of uranyl infrared spectroscopic properties in which a direct relationship between ν_3 and the U−O force constant is established;[67] this treatment is also applicable to other actinyls.

The IR results can be employed to evaluate the actinide−oxygen bond energies in actinyls. The bond dissociation energies (BDEs) of the dipositive actinyls are as follows: BDE[OU^{2+}−O] = 529 ± 31 kJ/mol; BDE[ONp^{2+}−O] = 504 ± 10 kJ/mol; BDE[OPu^{2+}−O] = 403 ± 95 kJ/mol.[12] The values for uranyl and neptunyl are roughly similar, while the uncertainty for the plutonyl BDE is too large to make a valid comparison. Cremer and co-workers have discussed that the BDE is not a direct measure of bond strength but rather that the intrinsic bond dissociation energy (IBDE) needs to be evaluated for this purpose.[68,69] In the case of a molecule AB, Kraka and Cremer define the IBDE as "the energy needed to separate two atoms A and B directly connected by a bond without changing their electronic features (degree of hybridization) and their bonds to other atoms, that is, apart from the bond being broken, the electronic structure of the fragments after bond breaking is the same as in the molecule."[70] The

concept and evaluation of intrinsic bond energy has been discussed for small transition metal, lanthanide and actinide molecules by Armentrout and others.[71−74] The IBDE, which is the indicator of the actual bonding between two atoms, cannot be directly experimentally determined because relaxation of the dissociated fragments, A and B, cannot be avoided. It is furthermore impractical to compute IBDEs because in the course of the computations, the fragments relax to low-energy states, just as they do in experiments. In general, the IBDE will be higher than the measured BDE due to stabilization (relaxation) of the fragments A and B upon dissociation of the A−B bond. Specifically, IBDE = BDE − relaxation energy, where the relaxation energy corresponds to a decrease in the energies of the dissociated fragments and is thus ≤0. In accord with early work by Gordy,[75] Kraka and Cremer[70] concluded that the harmonic stretching force constant is generally a reliable indicator of the IBDE, and thus the actual inherent bond strength. For the specific case of uranyl, this conclusion is in accord with the experimental results of Groenewold et al.[33,36] and the theoretical interpretations of Vallet et al.[26]

The inherent importance of IBDEs to the field of chemistry was discussed by Pauling in 1945.[76] Later, S. Siegel and B. Siegel provided the following concise statement of the importance of IBDE versus BDE (referred to by them as I and E, respectively):[77] "The discrepancy between models based on E and I stems from the fact that E values are based on the sum of internal energies of the isolated atoms and energy terms characteristic of the bond itself. It is the latter energy terms which determine the ground state bond properties of the molecule and not the contribution to the atomic heat of formation by the internal valence electrons of the isolated atoms." Armentrout et al.[72] evaluated the IBDEs for transition metal−carbon double bonds in M^+−CH_2, concluding that the IBDE is nearly constant, ca. 420 kJ/mol, whereas a BDE as low as 225 kJ/mol was measured for Cr^+−CH_2. These authors further pointed out that it is the IBDE that is useful in evaluating the maximum degree of bonding in condensed phase and interfacial systems. It was similarly demonstrated that the IBDEs of LnO molecules, where Ln is a lanthanide, are essentially constant across the lanthanide series while the BDEs vary from ca. 400 kJ/mol for YbO to ca. 1000 kJ/mol for LaO, the latter being the approximate IBDE for all of the LnO.[74] Despite the large variations in their BDEs, based on the nearly constant IBDEs for the LnO molecules it is predicted that condensed phase phenomena in which the Ln-O bonding is retained should be similar across the series. For example, the melting points of the lanthanide sesquioxides vary by only ca. 10% across the entire series and do not whatsoever correlate with the BDEs of the LnO.[78] With the exceptions of processes that involve breaking Ln−O bonds, the experimental BDEs of which vary substantially among the lanthanides, the condensed phase chemistry across the lanthanide oxide series is nearly invariant.

Both the experimental results for aqueous actinyl ions[16] and the present computational results for actinyl-TMOGA complexes indicate that the ν_3 frequencies vary little across the actinyl series, by less than 1%. The inferred force constants, which are proportional to ν_3^2,[67] thus vary by less than 2% (the small difference in masses of U-238, Np-237 and Pu-239 can be neglected). It can be assumed that the degree of electron donation from the TMOGA ligands is similar for all three $AnO_2(TMOGA)_2^{2+}$ such that all of the ν_3 values are similarly shifted relative to the bare AnO_2^{2+} ions. To the extent that the

force constants correlate with the IBDEs, we conclude that the IBDEs are very similar for UO_2^{2+}, NpO_2^{2+} and PuO_2^{2+}. Based on the BDEs cited above, the lowest BDE limits are $BDE[OU^{2+}−O] \geq 498$ kJ/mol, $BDE[ONp^{2+}−O] \geq 494$ kJ/mol and $BDE[OPu^{2+}−O] \geq 308$ kJ/mol. Considering the similarities of their force constants, the IBDEs for the three AnO_2^{2+} should be comparable and at least as large as the highest BDE: $IBDE \geq BDE[OU^{2+}−O] = 498$ kJ/mol. We thus assign a *lower limit* for the IBDEs of the three actinyls as ca. 500 kJ/mol; the actual IBDE may be significantly higher but, most importantly, is considered to be essentially the same for all three actinyls. A recent assessment of vibrational frequencies of uranyl and plutonyl compounds found similar ν_3 frequencies for isostructural compounds.[25] In that work, the small decreases in ν_3 from uranyl to plutonyl (neptunyl was not studied) were correlated with the experimental bond energies. The small (<3%) differences in ν_3 frequencies for selected uranyl and plutonyl compounds[25] contrasts with the minuscule (<0.5%) difference in ν_3 between aqueous UO_2^{2+} and PuO_2^{2+}.[16] It should be emphasized that a physical property measured absent the breaking of a bond should not necessarily exhibit a correlation with the BDE, but rather a correlation with the (unknown) IBDE, which reflects the inherent nature of the bonding, a property that remains essentially unaltered in such processes as (moderate) vibrational excitation.

The conclusion here that the IBDEs of the actinyls are essentially the same despite large differences in the BDEs is consistent with experimental results that had previously been considered "enigmatic". For example, it is known that UO_2^+ exhibits faster oxo-exchange in aqueous solution than does PuO_2^+,[79] this in apparent conflict with the much lower $BDE[OPu^+−O]$ versus $BDE[OU^+−O]$.[12] This same "enigmatic" result was recently demonstrated in the gas phase and rationalized by computation of the potential energy profiles for exchange, which exhibited a higher transition state barrier for PuO_2^+ versus UO_2^+.[39] The relatively small difference in the transition state energies (as compared with the BDEs) was rationalized based on different degrees of covlancy in the actinide-oxygen bonds upon proceeding across the series. This provides an illustration of the inability of BDEs to predict the efficiency of processes such as oxo-exchange, in which there is no net change in bonding between reactants and products. The similarity of the IBDEs of the actinyls is crucial to understanding their condensed phase chemistry, in accord with the considerations presented by Pauling and others.[69,72,76,77]

■ CONCLUSIONS

The IRMPD spectrum for the gas-phase $UO_2(TMOGA)_2^{2+}$ coordination complex was acquired. The computed IR frequencies are in good agreement with the experimental values, with a maximum deviation of 1.6% between the observed and computed (unscaled) frequencies. All vibrational modes were assigned to the equatorial TMOGA ligands, except for the uranyl ν_3 asymmetric stretch that is diagnostic of the U−O bond strength, specifically the intrinsic bond dissociation energy, which decreases with increasing donation of electron charge from Lewis base equatorial ligands to uranium in dipositive uranyl coordination complexes. The measured ν_3 of 965 cm^{-1} for $UO_2(TMOGA)_2^{2+}$ is significantly below the lowest previously measured value of 988 cm^{-1} for a gas-phase uranyl coordination complex, $UO_2(acetone)_4^{2+}$, and is comparable to fully solvated UO_2^{2+} in aqueous solution. Given the established correlation between equatorial ligand GB and the

degree of red-shifting of the uranyl ν_3 frequency, the present results indicate that two tridentate TMOGA ligands have an effective GB that is significantly greater than four monodentate acetone ligands. These results suggest the opportunity to acquire ν_3 frequencies for additional $UO_2(L)_n^{2+}$ complexes, where L are monodentate ligands with high gas-phase basicities, to better establish a correlation between ν_3 and ligand GBs. If a sufficiently consistent correlation is established, then measured ν_3 for uranyl complexes could be employed to infer unknown ligand GBs.

The good agreement between the experimental and computed IR spectra for $UO_2(TMOGA)_2^{2+}$ provides confidence in the accuracy of the computed spectra for $NpO_2(TMOGA)_2^{2+}$ and $PuO_2(TMOGA)_2^{2+}$. The computed ν_3 frequencies for the neptunyl and plutonyl complexes are similar, with the neptunyl value a few cm^{-1} higher than the other two. This is the same ν_3 relationship known for the aqueous dipositive actinyl ions: the values for uranyl and plutonyl are nearly the same, and a few cm^{-1} below that for neptunyl. Vibrational stretching frequencies can be used to derive force constants, which have been shown to correlate with intrinsic bond dissociation energies, an intangible quantity that represents the inherent bonding interactions in a molecule. The distinction between experimental BDEs and intrinsic BDEs is a crucial but often overlooked concept. The similarities among the ν_3 frequencies for uranyl, neptunyl, and plutonyl in comparable environments are taken to indicate that the intrinsic BDEs for OAn^{2+}−O are similar, to within less than 5%, for An = U, Np. and Pu. This conclusion has no bearing on the measured BDEs, which may exhibit substantially greater deviations among the actinyls.

Computations were also performed for the $UO_2(TMGA)_2^{2+}$ complex, where TMGA is the ligand in which the central O$_{ether}$ of TMOGA has been replaced by a CH$_2$ moiety. The unexpected result was that the predicted ν_3 for $UO_2(TMOGA)_2^{2+}$ and $UO_2(TMGA)_2^{2+}$ are essentially the same to within a few cm^{-1}. This result suggests that the interaction of the O$_{ether}$ atom with uranium is minimal and that the coordination in $UO_2(TMOGA)_2^{2+}$ is dominated by interactions with the O$_{carboxylate}$ atoms. Based on this result, it is predicted that the net electron donation, and thus ν_3, should be similar for uranyl coordinated by two TMOGA ligands or by four dimethylformamide ligands.

■ AUTHOR INFORMATION

Corresponding Authors
*E-mail: jkgibson@lbl.gov.
*E-mail: junli@tsinghua.edu.cn.

Notes
The authors declare no competing financial interest.

■ REFERENCES

(1) Ahrland, S. On the Complex Chemistry of the Uranyl Ion 0.1. The Hydrolysis of the 6-Valent Uranium in Aqueous Solutions. *Acta Chem. Scand.* **1949**, *3*, 374−400.

(2) Crandall, H. W. The Formula of Uranyl Ion. *J. Chem. Phys.* **1949**, *17*, 602−606.

(3) Denning, R. G. Electronic-Structure and Bonding in Actinyl Ions. *Struct. Bonding (Berlin)* **1992**, *79*, 215−276.

(4) Denning, R. G. Electronic Structure and Bonding in Actinyl Ions and Their Analogs. *J. Phys. Chem. A* **2007**, *111*, 4125−4143.

(5) Clark, D. L.; Conradson, S. D.; Donohoe, R. J.; Keogh, D. W.; Morris, D. E.; Palmer, P. D.; Rogers, R. D.; Tait, C. D. Chemical Speciation of the Uranyl Ion Under Highly Alkaline Conditions. Synthesis, Structures, and Oxo Ligand Exchange Dynamics. *Inorg. Chem.* **1999**, *38*, 1456−1466.

(6) Neidig, M. L.; Clark, D. L.; Martin, R. L. Covalency in F-Element Complexes. *Coord. Chem. Rev.* **2013**, *257*, 394−406.

(7) Baker, R. J. New Reactivity of the Uranyl(VI) Ion. *Chem.—Eur. J.* **2012**, *18*, 16258−16271.

(8) Bühl, M.; Wipff, G. Insights into Uranyl Chemistry from Molecular Dynamics Simulations. *ChemPhysChem* **2011**, *12*, 3095−3105.

(9) Fortier, S.; Hayton, T. W. Oxo Ligand Functionalization in the Uranyl Ion (UO$_2^{2+}$). *Coord. Chem. Rev.* **2010**, *254*, 197−214.

(10) Jorgensen, C. K.; Reisfeld, R. Uranyl Photophysics. *Struct. Bonding (Berlin)* **1982**, *50*, 121−171.

(11) Infante, I.; Kovacs, A.; La Macchia, G.; Shahi, A. R. M.; Gibson, J. K.; Gagliardi, L. Ionization Energies for the Actinide Mono- and Dioxides Series, from Th to Cm: Theory versus Experiment. *J. Phys. Chem. A* **2010**, *114*, 6007−6015.

(12) Marçalo, J.; Gibson, J. K. Gas-Phase Energetics of Actinide Oxides: An Assessment of Neutral and Cationic Monoxides and Dioxides from Thorium to Curium. *J. Phys. Chem. A* **2009**, *113*, 12599−12606.

(13) Cornehl, H. H.; Heinemann, C.; Marçalo, J.; Pires de Matos, A.; Schwarz, H. The "Bare" Uranyl^{2+} Ion, UO$_2^{2+}$. *Angew. Chem., Int. Ed.* **1996**, *35*, 891−894.

(14) Shamov, G. A.; Schreckenbach, G. Theoretical Study of the Oxygen Exchange in Uranyl Hydroxide. An Old Riddle Solved? *J. Am. Chem. Soc.* **2008**, *130*, 13735−13744.

(15) Bühl, M.; Schreckenbach, G. Oxygen Exchange in Uranyl Hydroxide via Two "Nonclassical" Ions. *Inorg. Chem.* **2010**, *49*, 3821−3827.

(16) Jones, L. H.; Penneman, R. A. Infrared Spectra and Structure of Uranyl and Transuranium (V) and (VI) Ions in Aqueous Perchloric Acid Solution. *J. Chem. Phys.* **1953**, *21*, 542−544.

(17) Jung, W. S.; Tomiyasu, H.; Fukutomi, H. Influence of the Base Strength of Ligand on Infrared-Spectra of Uranyl(VI) Complexes in Solution. *Bull. Korean Chem. Soc.* **1985**, *6*, 318−319.

(18) Gal, M.; Goggin, P. L.; Mink, J. Vibrational Spectroscopic Studies of Uranyl Complexes in Aqueous and Nonaqueous Solutions. *Spectrochim. Acta, Part A* **1992**, *48*, 121−132.

(19) Gal, M.; Goggin, P. L.; Mink, J. Mid-Infrared, Far-Infrared and Raman-Spectra of Uranyl Complexes in Aqueous-Solutions. *J. Mol. Struct.* **1984**, *114*, 459−462.

(20) Mcglynn, S. P.; Neely, W. C.; Smith, J. K. Electronic Structure, Spectra, and Magnetic Properties of Oxycations 0.3. Ligation Effects on Infrared Spectrum of Uranyl Ion. *J. Chem. Phys.* **1961**, *35*, 105−116.

(21) Tanaka, Y.; Fukuda, J.; Okamoto, M.; Maeda, M. Infrared Spectroscopic and Chromatographic Studies on Uranium Isotope Effect in Formation of Uranyl Acetate, Citrate and Fluoride Complexes in Aqueous-Solution. *J. Inorg. Nucl. Chem.* **1981**, *43*, 3291−3294.

(22) Bray, R. G.; Kramer, G. M. Correlation of Spectroscopic Parameters with Ligand Basicity for Uranyl Bis-(Hexafluoroacetylacetonate) Adducts. *Inorg. Chem.* **1983**, *22*, 1843−1848.

(23) Quiles, F.; Burneau, A. Infrared and Raman Spectroscopic Study of Uranyl Complexes: Hydroxide and Acetate Derivatives in Aqueous Solution. *Vib. Spectrosc.* **1998**, *18*, 61−75.

(24) Forbes, T. Z.; Goss, V.; Jain, M.; Burns, P. C. Structure Determination and Infrared Spectroscopy of $K(UO_2)(SO_4)(OH)(H-O\cdot 2)$ and $K(UO_2)(SO_4)(OH)$. *Inorg. Chem.* **2007**, *46*, 7163−7168.

(25) Schnaars, D. D.; Wilson, R. E. Structural and Vibrational Properties of $U(VI)O_2Cl_4^{2-}$ and $Pu(VI)O_2Cl_4^{2-}$ Complexes. *Inorg. Chem.* **2013**, *52*, 14138−14147.

(26) Vallet, V.; Wahlgren, U.; Grenthe, I. Probing the Nature of Chemical Bonding in Uranyl(VI) Complexes with Quantum Chemical Methods. *J. Phys. Chem. A* **2012**, *116*, 12373−12380.

(27) Bühl, M.; Sieffert, N.; Chaumont, A.; Wipff, G. Water versus Acetonitrile Coordination to Uranyl. Density Functional Study of Cooperative Polarization Effects in Solution. *Inorg. Chem.* **2011**, *50*, 299−308.

(28) Hunt, R. D.; Andrews, L. Reactions of Pulsed-Laser Evaporated Uranium Atoms with Molecular-Oxygen - Infrared-Spectra of UO, UO_2, UO_3, UO_2^+, UO_2^{2+}, and UO_3-O_2 in Solid Argon. *J. Chem. Phys.* **1993**, *98*, 3690−3696.

(29) Zhou, M. F.; Andrews, L.; Ismail, N.; Marsden, C. Infrared Spectra of UO_2, UO_2^+, and UO_2^- in Solid Neon. *J. Phys. Chem. A* **2000**, *104*, 5495−5502.

(30) Li, J.; Bursten, B. E.; Andrews, L.; Marsden, C. J. On the Electronic Structure of Molecular UO_2 in the Presence of Ar Atoms: Evidence for Direct U-Ar Bonding. *J. Am. Chem. Soc.* **2004**, *126*, 3424−3425.

(31) Wang, X. F.; Andrews, L.; Li, J.; Bursten, B. E. Significant Interactions Between Uranium and Noble-Gas Atoms: Coordination of the UO_2^+ Cation by Ne, Ar, Kr, and Xe Atoms. *Angew. Chem., Int. Ed.* **2004**, *43*, 2554−2557.

(32) Lias, S. G.; Bartmess, J. E.; Liebman, J. F.; Holmes, J. L.; Levin, R. D.; Mallard, W. G. In *NIST Chemistry WebBook*; NIST Standard Reference Database Number 69; Linstrom, P. J., Mallard, W. G., Eds.; National Institute of Standards and Technology: Gaitherburg, MD, 2014.

(33) Groenewold, G. S.; Oomens, J.; de Jong, W. A.; Gresham, G. L.; McIlwain, M. E.; Van Stipdonk, M. J. Vibrational Spectroscopy of Anionic Nitrate Complexes of UO_2^{2+} and Eu^{3+} Isolated in the Gas Phase. *Phys. Chem. Chem. Phys.* **2008**, *10*, 1192−1202.

(34) Groenewold, G. S.; van Stipdonk, M. J.; Oomens, J.; de Jong, W. A.; Gresham, G. L.; McIlwain, M. E. Vibrational Spectra of Discrete UO_2^{2+} Halide Complexes in the Gas Phase. *Int. J. Mass Spectrom.* **2010**, *297*, 67−75.

(35) Groenewold, G. S.; de Jong, W. A.; Oomens, J.; Van Stipdonk, M. J. Variable Denticity in Carboxylate Binding to the Uranyl Coordination Complexes. *J. Am. Soc. Mass Spectrom.* **2010**, *21*, 719−727.

(36) Groenewold, G. S.; Gianotto, A. K.; Cossel, K. C.; Van Stipdonk, M. J.; Moore, D. T.; Polfer, N.; Oomens, J.; de Jong, W. A.; Visscher, L. Vibrational Spectroscopy of Mass-Selected $[UO_2(ligand)_n]^{2+}$ Complexes in the Gas Phase: Comparison with Theory. *J. Am. Chem. Soc.* **2006**, *128*, 4802−4813.

(37) Valle, J. J.; Eyler, J. R.; Oomens, J.; Moore, D. T.; van der Meer, A. F. G.; von Helden, G.; Meijer, G.; Hendrickson, C. L.; Marshall, A. G.; Blakney, G. T. Free Electron Laser-Fourier Transform Ion Cyclotron Resonance Mass Spectrometry Facility for Obtaining Infrared Multiphoton Dissociation Spectra of Gaseous Ions. *Rev. Sci. Instrum.* **2005**, *76*, 0231031−0231037.

(38) Su, J.; Zhang, K.; Schwarz, W. H. E.; Li, J. Uranyl−Glycine−Water Complexes in Solution: Comprehensive Computational Modeling of Coordination Geometries, Stabilization Energies, and Luminescence Properties. *Inorg. Chem.* **2011**, *50*, 2082−2093.

(39) Rios, D.; Michelini, M. C.; Lucena, A. F.; Marçalo, J.; Gibson, J. K. On the Origins of Faster Oxo Exchange for Uranyl(V) versus Plutonyl(V). *J. Am. Chem. Soc.* **2012**, *134*, 15488−15496.

(40) Tian, G. X.; Rao, L. F.; Teat, S. J.; Liu, G. K. Quest for Environmentally Benign Ligands for Actinide Separations: Thermodynamic, Spectroscopic, and Structural Characterization of U-VI Complexes with Oxa-Diamide and Related Ligands. *Chem.—Eur. J.* **2009**, *15*, 4172−4181.

(41) Rao, L. F.; Tian, G. X.; Teat, S. J. Complexation of Np(V) with N,N-dimethyl-3-oxa-glutaramic Acid and Related Ligands: Thermodynamics, Optical Properties and Structural Aspects. *Dalton Trans.* **2010**, *39*, 3326−3330.

(42) Tian, G. X.; Teat, S. J.; Rao, L. F. Structural and Thermodynamic Study of the Complexes of Nd(III) with N,N,N′,N′-Tetramethyl-3-oxa-glutaramide and the Acid Analogues. *Inorg. Chem.* **2014**, *53*, 9477−9485.

(43) Tian, G. X.; Teat, S. J.; Rao, L. F. Formation, Structure, and Optical Properties of PuO_2^{2+} Complexes with N,N,N′,N′-tetramethyl-3-oxa-glutaramide. *Inorg. Chem. Commun.* **2014**, *44*, 32−36.

(44) Gong, Y.; Hu, H. S.; Tian, G. X.; Rao, L. F.; Li, J.; Gibson, J. K. A Tetrapositive Metal Ion in the Gas Phase: Thorium(IV) Coordinated by Neutral Tridentate Ligands. *Angew. Chem., Int. Ed.* **2013**, *52*, 6885−6888.

(45) Gong, Y.; Tian, G. X.; Rao, L. F.; Gibson, J. K. Tetrapositive Plutonium, Neptunium, Uranium, and Thorium Coordination Complexes: Chemistry Revealed by Electron Transfer and Collision Induced Dissociation. *J. Phys. Chem. A* **2014**, *118*, 2749−2755.

(46) Gong, Y.; Hu, H. S.; Rao, L. F.; Li, J.; Gibson, J. K. Experimental and Theoretical Studies on the Fragmentation of Gas-Phase Uranyl−, Neptunyl−, and Plutonyl−Diglycolamide Complexes. *J. Phys. Chem. A* **2013**, *117*, 10544−10550.

(47) Groenewold, G. S.; van Stipdonk, M. J.; Oomens, J.; de Jong, W. A.; McIlwain, M. E. The Gas-Phase bis-Uranyl Nitrate Complex $[(UO_2)_2(NO_3)_5]^−$: Infrared Spectrum and Structure. *Int. J. Mass Spectrom.* **2011**, *308*, 175−180.

(48) Dain, R. P.; Gresham, G.; Groenewold, G. S.; Steill, J. D.; Oomens, J.; van Stipdonk, M. J. Infrared Multiple-Photon Dissociation Spectroscopy of Group II Metal Complexes with Salicylate. *Rapid Commun. Mass Spectrom.* **2011**, *25*, 1837−1846.

(49) Dain, R. P.; Gresham, G.; Groenewold, G. S.; Steill, J. D.; Oomens, J.; Van Stipdonk, M. J. Infrared Multiple Photon Dissociation Spectroscopy of Group I and Group II Metal Complexes with BOC-Hydroxylamine. *Rapid Commun. Mass Spectrom.* **2013**, *27*, 1867−1872.

(50) Bagratashvili, V. N.; Letokov, V. A.; Makarov, A. A.; Ryabov, E. A. In *Multiple Photon Infrared Laser Photophysics and Photochemistry*; Harwood Chur: Switzerland, 1985.

(51) Oomens, J.; Tielens, A. G. G. M.; Sartakov, B. G.; von Helden, G.; Meijer, G. Laboratory Infrared Spectroscopy of Cationic Polycyclic Aromatic Hydrocarbon Molecules. *Astrophys. J.* **2003**, *591*, 968−985.

(52) Moore, D. T.; Oomens, J.; Eyler, J. R.; von Helden, G.; Meijer, G.; Dunbar, R. C. Infrared Spectroscopy of Gas-Phase Cr^+ Coordination Complexes: Determination of Binding Sites and Electronic States. *J. Am. Chem. Soc.* **2005**, *127*, 7243−7254.

(53) Hohenberg, P.; Kohn, W. Inhomogeneous Electron Gas. *Phys. Rev. B* **1964**, *136*, B864−B871.

(54) Kohn, W.; Sham, L. J. Self-Consistent Equations Including Exchange and Correlation Effects. *Phys. Rev.* **1965**, *140*, A1133−A1138.

(55) Dirac, P. A. M. Note on Exchange Phenomena in the Thomas Atom. *Proc. Cambridge Philos. Soc.* **1930**, *26*, 376−385.

(56) Vosko, S. H.; Wilk, L.; Nusair, M. Accurate Spin-Dependent Electron Liquid Correlation Energies for Local Spin-Density Calculations - A Critical Analysis. *Can. J. Phys.* **1980**, *58*, 1200−1211.

(57) Perdew, J. P.; Burke, K.; Ernzerhof, M. Generalized Gradient Approximation Made Simple. *Phys. Rev. Lett.* **1996**, *77*, 3865−3868.

(58) *ADF 2010.01, SCM, Theoretical Chemistry*; Vrije Universiteit: Amsterdam, The Netherlands.

(59) Fonseca Guerra, C.; Snijders, J. G.; te Velde, G.; Baerends, E. J. Towards an Order-N DFT Method. *Theor. Chem. Acc.* **1998**, *99*, 391−403.

(60) te Velde, G.; Bickelhaupt, F. M.; Baerends, E. J.; Fonseca Guerra, C.; Van Gisbergen, S. J. A.; Snijders, J. G.; Ziegler, T. Chemistry with ADF. *J. Comput. Chem.* **2001**, *22*, 931−967.

(61) Van Lenthe, E.; Baerends, E. J.; Snijders, J. G. Relativistic Regular 2-Component Hamiltonians. *J. Chem. Phys.* **1993**, *99*, 4597−4610.

(62) Van Lenthe, E.; Baerends, E. J. Optimized Slater-Type Basis Sets for the Elements 1−118. *J. Comput. Chem.* **2003**, *24*, 1142−1156.

(63) Gorllerwalrand, C.; Colen, W. On the Coordination Symmetry of the Hydrated Uranyl-Ion. *Chem. Phys. Lett.* **1982**, *93*, 82−85.

(64) Neuefeind, J.; Soderholm, L.; Skanthakumar, S. Experimental Coordination Environment of Uranyl(VI) in Aqueous Solution. *J. Phys. Chem. A* **2004**, *108*, 2733−2739.

(65) Thompson, H. A.; Brown, G. E.; Parks, G. A. XAFS Spectroscopic Study of Uranyl Coordination in Solids and Aqueous Solution. *Am. Mineral.* **1997**, *82*, 483−496.

(66) Jones, L. H. Systematics in the Vibrational Spectra of Uranyl Complexes. *Spectrochim. Acta* **1958**, *10*, 395−403.

(67) Rabinowitch, E. *Spectroscopy of Uranyl Salts in the Solid State*; U.S. Atomic Energy Commission: Washington, DC, 1953.

(68) Larsson, J. A.; Cremer, D. Theoretical Verification and Extension of the McKean Relationship Between Bond Lengths and Stretching Frequencies. *J. Mol. Struct.* **1999**, *485*, 385−407.

(69) Cremer, D.; Wu, A. N.; Larsson, A.; Kraka, E. Some Thoughts About Bond Energies, Bond Lengths, and Force Constants. *J. Mol. Model.* **2000**, *6*, 396−412.

(70) Kraka, E.; Cremer, D. Characterization of CF Bonds with Multiple-Bond Character: Bond Lengths, Stretching Force Constants, and Bond Dissociation Energies. *ChemPhysChem* **2009**, *10*, 686−698.

(71) Schilling, J. B.; Beauchamp, J. L. Hydrocarbon Activation by Gas-Phase Lanthanide Cations - Interaction of Pr^+, Eu^+, and Gd^+ with Small Alkanes, Cycloalkanes, and Alkenes. *J. Am. Chem. Soc.* **1988**, *110*, 15−24.

(72) Armentrout, P. B.; Sunderlin, L. S.; Fisher, E. R. Intrinsic Transition-Metal Carbon Double-Bond Dissociation-Energies - Periodic Trends in M^+−CH_2 Bond Strengths. *Inorg. Chem.* **1989**, *28*, 4436−4437.

(73) Sunderlin, L. S.; Armentrout, P. B. Periodic Trends in Chemical-Reactivity - Reactions of Sc^+, Y^+, La^+, and Lu^+ with Methane and Ethane. *J. Am. Chem. Soc.* **1989**, *111*, 3845−3855.

(74) Gibson, J. K. Role of Atomic Electronics in F-Element Bond Formation: Bond Energies of Lanthanide and Actinide Oxide Molecules. *J. Phys. Chem. A* **2003**, *107*, 7891−7899.

(75) Gordy, W. A Relation between Bond Force Constants, Bond Orders, Bond Lengths, and the Electronegativities of the Bonded Atoms. *J. Chem. Phys.* **1946**, *14*, 305−320.

(76) Pauling, L. The Valence-State Energy of the Bivalent Oxygen Atom. *Proc. Natl. Acad. Sci. U.S.A.* **1949**, *35*, 229−232.

(77) Siegel, S.; Siegel, B. Intrisic Bond Energies. *J. Chem. Educ.* **1963**, *40*, 143−145.

(78) Zinkevich, M. Thermodynamics of Rare Earth Sesquioxides. *Prog. Mater. Sci.* **2007**, *52*, 597−647.

(79) Rabideau, S. W.; Masters, B. J. Oxygen Exchange Reactions of Plutonium Ions in Solution. *J. Phys. Chem.* **1963**, *67*, 318−323.